BRILL

Nematology 18 (2016) 697-709

Nematology
brill.com/nemy

Characterization of glutathione S-transferases from the pine wood nematode, *Bursaphelenchus xylophilus*

Margarida ESPADA [1,2], John T. JONES [2,3] and Manuel MOTA [1,4,*]

[1] *NemaLab/ICAAM – Instituto de Ciências Agrárias e Ambientais Mediterrânicas, Universidade de Évora, Núcleo da Mitra, Ap. 94, 7002-554 Évora, Portugal*
[2] *Cell and Molecular Sciences Group, The James Hutton Institute, Invergowrie, Dundee DD2 5DA, UK*
[3] *School of Biology, University of St Andrews, North Haugh, St Andrews KY16 9TZ, UK*
[4] *Departamento de Ciências da Vida, Universidade Lusófona de Humanidades e Tecnologias, EPCV, C. Grande 376, 1749-024 Lisbon, Portugal*

Received: 29 January 2016; revised: 5 April 2016
Accepted for publication: 7 April 2016; available online: 10 May 2016

Summary – We have previously identified two secreted glutathione S-transferases (GST) expressed in the pharyngeal gland cell of *Bursaphelenchus xylophilus*, which are upregulated post infection of the host. This study examines the functional role of GSTs in *B. xylophilus* biology. We analysed the expression profiles of all predicted GSTs in the genome and the results showed that they belong to kappa and cytosolic subfamilies and the majority are upregulated post infection of the host. A small percentage is potentially secreted and none is downregulated post infection of the host. One secreted protein was confirmed as a functional GST and is within a cluster that showed the highest expression fold change in infection. This enzyme has a protective activity that may involve host defences, namely in the presence of terpenoid compounds and peroxide products. These results suggest that GSTs secreted into the host participate in the detoxification of host-derived defence compounds and enable successful parasitism.

Keywords – detoxification metabolism, effectors, plant-parasitic nematode, terpenoid compounds.

Glutathione S-transferases (GST, EC 2.5.1.18) are enzymes involved in detoxification metabolism and are present in a range of different organisms including bacteria, plants and animals. The main function of this large family of enzymes is the detoxification of potentially damaging endogenous stress products and exogenous xenobiotic compounds, and also an important role in drug metabolism. This is achieved by the ability to catalyse the conjugation of the reduced form of glutathione (GSH) to potential toxins in order to increase their solubility and thus enable them to be metabolised or excreted from the host (Brophy & Pritchard, 1994; Campbell *et al*., 2001; Torres-Rivera & Landa, 2008; Matoušková *et al*., 2016). GST does not act directly on reactive oxygen species (ROS), but on the oxidised products of their activity, including lipid hydroperoxides and reactive carbonyls (Torres-Rivera & Landa, 2008). In parasitic species GST is an important detoxification enzyme, especially in helminths where GSTs provide initial defence against oxidative damage and protect the worm from the host immune response, as well as acting as drug-binding proteins (Precious & Barrett, 1989; Brophy & Barrett, 1990; Brophy & Pritchard, 1994; Matoušková *et al*., 2016). Therefore, the roles of these enzymes in the host-parasite interaction have been studied extensively. Recent studies on GSTs from animal-parasitic helminths showed that sigma-GSTs have prostaglandin synthase activity, and bind to toxins as a suppression of the host immune response to the benefit of the parasite (van Rossum *et al*., 2004; Dowling *et al*., 2010; LaCourse *et al*., 2012). In addition, analysis of the secretome of the animal-parasitic trematode *Fasciola hepatica*, revealed sigma class-GST in extracellular vesicules that are deployed during parasitism (Cwiklinski *et al*., 2015). In the plant-parasitic nematode *Meloidogyne incognita*, one GST has been identified as being secreted from the pharyngeal gland cells (*Mi-gst-1*) and plays an important role in the interaction with the host as evidenced by the fact that silencing of this gene by RNAi leads to a reduction in parasitism. This GST may protect the nematode against host-derived ROS or may

* Corresponding author, e-mail: mmota@uevora.pt

© Koninklijke Brill NV, Leiden, 2016
DOI 10.1163/15685411-00002985

modulate plant responses that are triggered by nematode attack (Dubreuil *et al*., 2007).

Parasitic helminths contain several forms of GSTs that can be grouped in subfamilies on the basis of their subcellular location: kappa (mitochondrial), microsomal and cytosolic (soluble GSTs from the mu, alpha, pi, theta, sigma, zeta and omega classes) (Frova, 2006; Torres-Rivera & Landa, 2008). Several GSTs have been identified in migratory plant-parasitic nematodes, including *Bursaphelenchus xylophilus*, *Ditylenchus africanus*, *Pratylenchus coffeae*, *Radopholus similis* and from the sedentary species *Meloidogyne* spp. and *Globodera pallida* (Dubreuil *et al*., 2007; Bellafiore *et al*., 2008; Jacob *et al*., 2008; Haegeman *et al*., 2009, 2011; Kikuchi *et al*., 2011; Cotton *et al*., 2014; Espada *et al*., 2016). A total of 65 potential GSTs were predicted from the genome of *B. xylophilus*, a similar number to that in *Caenorhabditis elegans*, but higher than seen in other plant-parasitic nematodes (Kikuchi *et al*., 2011).

When the pine wood nematode (PWN) *B. xylophilus* infects a tree it triggers several physical and chemical alterations leading to the symptoms of pine wilt disease (PWD). Kuroda *et al*. (1991) hypothesised a mechanism of cavitation, in which terpenoids synthesised in xylem ray cells induce cavitation and embolisms in tracheids leading to failure of water transport. Previous studies have shown that levels of plant terpenes in *Pinus thunbergii*, particularly α-pinene and β-pinene, increase when the tree is infected by *B. xylophilus* (Kuroda, 1991; Kuroda *et al*., 1991; Fukuda *et al*., 1997). However, a recent study examining infection of plant material maintained in tissue culture suggested that terpenoid compounds do not significantly increase after infection with PWN although levels were maintained after infection, with α-pinene making up between 26-32% of total terpenoid content and β-pinene between 34-47% (Faria *et al*., 2015). Several of these compounds have nematicidal activity, although no study has been made in *B. xylophilus*. Chemical compounds including terpenoids have been tested against filarial nematode GST and one study showed that α-pinene has an inhibitory effect on the nematode GST (Azeez *et al*., 2012).

In a previous study, we identified two secreted glutathione S-transferases that were upregulated in an early stage of infection and which are expressed in the dorsal pharyngeal gland cell (Espada *et al*., 2016). It was suggested that these enzymes could be involved in detoxification of plant endogenous compounds, helping *B. xylophilus* to overcome host defences. Here we demonstrate that at least one of these is a functional GST and that the presence of this enzyme provides protection against stresses likely to be encountered during infection of the host tree. We show that biochemically active GST is secreted by nematodes. In addition, we examine the global changes in expression of *B. xylophilus* GSTs upon infection of the host.

Materials and methods

Phylogenetic analysis of GST sequences

Potential GST-encoding sequences were identified using the previous data from Kikuchi *et al*. (2011) and by BLASTP searching the gene calls from the *B. xylophilus* genome against the NR database (cutoff $1e^{-5}$). Any sequences for which at least one of the top three hits included the expression "glutathione S-transferase" were selected for further analysis. This analysis was performed using BLAST+ wrappers for Galaxy (v0.1.01) (Cock *et al*., 2015). The expression levels of the transcripts at various life stages were predicted from RNAseq data generated in a previous study (Espada *et al*., 2016) and $\log_2$ of the fold change for each gene was calculated. For all the predicted GSTs the subfamilies and protein domains were identified using InterProScan 5 (Jones *et al*., 2014) (http://www.ebi.ac.uk/interpro/search/sequence-search). Secreted GSTs were predicted based on the presence of signal peptide as predicted by SignalP (v3.0) (Bendtsen *et al*., 2004) and the absence of a transmembrane domain. All the alignments of the full-length protein sequences were performed with the software SeaView (Gouy *et al*., 2010). The Maximum-likelihood phylogenetic tree was generated by PhyML (in SeaView) from the alignment of the sequences (protein distance measure: Jukes-cantor; aLRT SH-like for branch supporting). The phylogenetic tree was edited in FigTree (v1.4.0) (http://tree.bio.ed.ac.uk/software/figtree/). A neighbour-joining phylogenetic tree was generated in the software CLC Sequence Viewer (v7.6.1) (protein distance measure: Jukes-cantor; one thousand replicates for bootstrap for branch supporting).

Biological material

Nematodes were cultured on *Botrytis cinerea* and harvested using a Baermann funnel as previously described (Espada *et al*., 2016). Secreted proteins were collected as described in Kikuchi *et al*. (2004). Briefly, mixed life-stage nematodes were collected in a 15-ml tube, by centrifugation at 2844 *g* for 15 min, suspended in 1 ml M9

buffer and incubated for 2 days at 18°C. Thereafter the sample was centrifuged at 2844 *g* to pellet the nematodes, the supernatant containing secreted proteins was collected and stored in aliquots at −80°C until used in enzyme assays.

Cloning in expression vector and protein purification

The primers to amplify the full-length of one of the *B. xylophilus* GSTs shown to be expressed in the dorsal pharyngeal gland cells (BUX.s00647.112) were designed from the cDNA sequence lacking the signal peptide (as predicted by SignalP 3.0). The gene specific primers included the Kozak sequence (ACCATG) in the forward primer (5′ACCATGTTAGAGCTGTATTATTTCAACGA GAAG) and a Stop codon (TGA) in the reverse primer (5′TGATTGAGTGGCATTGAAATAATTGTAAATCG). The full length gene was amplified using KOD Hot Start proof-reading DNA polymerase and purified using the QIAquick gel extraction Kit (Qiagen). The gene was cloned into the pCR8 TOPO vector and transformed in one shot TOP10 competent cells following the manufacturer's instructions (Invitrogen). The recombinant clones were screened by colony PCR and one clone was confirmed by sequencing. Purified entry plasmid (approximately 140 ng) was transferred to the destination vector pJC40 (a 10× His-tag N-terminus fusion vector) using the LR cloning kit following the manufacturer's instructions (Invitrogen). The cloning reaction was transformed into BL21(DE3) chemical competent cells. Positive transformants (construct pJC40 + 00647.112) were analysed by colony PCR and confirmed by sequencing. The His-tagged protein was induced by adding 1 mM IPTG (isopropyl-beta-D-thiogalactopyranoside) to a bacterial culture grown from a single colony in 10 ml LB with 100 μg ml^{-1} ampicillin at 37°C until the concentration reached an OD_{600} of 0.6. The protein was then purified using Ni-NTA resin columns (Ni-NTA Spin kit, Qiagen) following the manufacturer's protocol.

Resistance test in BL21(DE3) cells

To induce expression of the recombinant protein, a single colony was grown in 45 ml LB and 100 μg ml^{-1} of ampicillin at 37°C with agitation until the concentration reached an OD_{600} of 0.6. At this point 100 μl aliquots of the bacterial suspension were placed in new sterile 15 ml tubes containing 4 ml LB and to which the terpenes (limonene, (+) and (−)-α-pinene, (−)-β-pinene) or hydrogen peroxide were added. For each treatment, two different concentrations were tested and two replicates were used: 0.5% and 1% for limonene, (+) and (−)-α-pinene, (−)-β-pinene (Sigma-Aldrich); 1% and 3% for hydrogen peroxide. Protein expression was induced in the remaining bacterial suspension by adding 0.5 mM IPTG and incubating at 37°C, with agitation, for 2 h. After this time the terpenoid and hydrogen peroxide treatments were repeated using 100 μl aliquots of the bacterial suspension as described above. The respective control tubes were also grown in the same conditions. All the treatments were subsequently grown overnight at 37°C with agitation. The OD_{600} was measured for all treatments in a spectrophotometer (Spekol 1500, Analytik Jena). The results were analysed with an ANOVA test using the statistical software GenStat (version 17; VSN International, 2012).

Western blotting

Aliquots of the bacterial cells from test described above were used in a Western blot using an antibody against a poly-histidine tag (Sigma-Aldrich) to demonstrate the presence of the recombinant protein in the assay. The bacterial extracts were heated at 90°C for 10 min in NuPage LDS sample buffer (Invitrogen). The proteins were separated on a 4-12% NuPage Bis-Tris gel (Invitrogen) and transferred to nitrocellulose membrane (GE Healthcare). Immuno-detection of the protein was performed using anti-His antibody (Sigma) at 1:5000 dilution as primary antibody and detected using a secondary antibody conjugated to peroxidase (α-mouse IgGxHRP at 1:50 000) (Sigma) by chemiluminescence using the Pierce Supersignal West Pico kit (Thermo-Scientific).

Enzyme assay

The glutathione-S-transferase assay kit (Sigma-Aldrich) was used with 1-chloro-2,4-dinitrobenzene (CDNB) as the standard substrate to test activity of recombinant protein and activity present in collected secretions. All assays were replicated three times. A solution containing 2 mM reduced L-glutathione and 1 mM CNDB in Dulbecco's phosphate buffered saline was prepared and used within an hour of preparation; 50 μl aliquots of this solution were mixed with 1 μl of control GST enzyme or with test enzyme preparations and transferred to a quartz cuvette. Absorbance was measured at 340 nm, for 30 s each over a period of 5 min, after a lag time of 1 min, following the manufacturer's procedure. GST activity was calculated for each sample as described by the kit manufacturer.

Results and discussion

Global analysis of *B. xylophilus* GST expression profiles

An analysis of GSTs performed as part of the *B. xylophilus* genome project (Kikuchi *et al.*, 2011) identified 65 potential GSTs. Our BLASTP based analysis of the *B. xylophilus* genome revealed that five more sequences, which could encode proteins similar to GSTs, were present (Fig. 1). Analysis of the protein domains present in each sequence confirmed all the protein sequences as GSTs, as shown in the supplementary table (Table S1 in the Supplementary material). The majority of these sequences have a thioredoxin-like fold domain (IPR012336) followed by glutathione S-transferase N-terminal and C-terminal domains, both of which are features of a cytosolic subfamily (reviewed in Frova, 2006). Five sequences contained domains similar to maleylacetoacetate isomerase (IPR005955), which is a feature of the zeta class of GSTs. The other four sequences were identified as kappa subfamily GSTs, due to the presence of the DSBA-like thioredoxin domain (IPR01853) (a feature

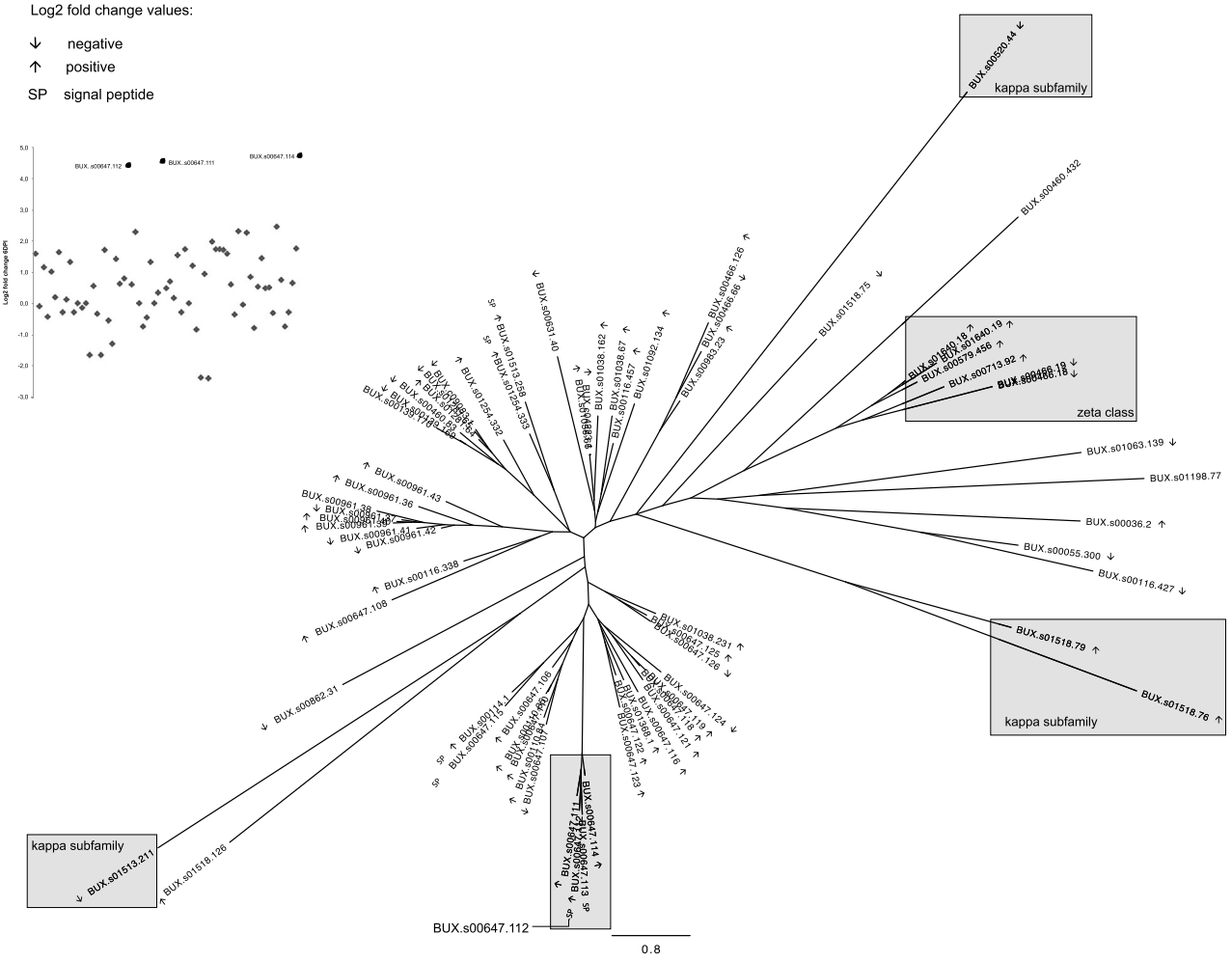

Fig. 1. Maximum-likelihood phylogenetic tree that represents the protein sequence similarity between all 70 *Bursaphelenchus xylophilus* predicted GSTs. The GSTs belonging to the kappa subfamily and to the cytosolic zeta class are represented within grey boxes. For each gene the $\log_2$ of the fold changes (6 days post infection) values of the expression levels are represented by arrows. The highest $\log_2$ fold change values belong to the genes BUX.s00647.112, BUX.s00647.111 and BUX.s00647.114 that cluster together (grey box). The dot plot on the top left of the figure is a representative chart of the expression values of all genes. SP represents the presence of a signal peptide.

of the HCCA isomerase/GST kappa family – IPR01440) (Frova, 2006).

Six of the GST sequences have a predicted signal peptide, suggesting a role in detoxification of extracellular compounds, including host-derived toxins (Fig. 1). These potentially secreted proteins included the two sequences (BUX.s00647.112 and BUX.s01254.333) that were previously identified as being expressed in the pharyngeal gland cells (Espada *et al*., 2016). Next we used our previously described RNAseq dataset to examine global changes in expression profiles of the GST sequences, by using $\log_2$ of the fold changes. This showed that 42 of the GST sequences are upregulated in nematodes after infection of trees as compared to nematodes grown on fungi (Fig. 1), including four of those sequences with a signal peptide. None of the secreted GSTs was downregulated after infection. The maximum-likelihood phylogenetic analysis (Fig. 1) of the *B. xylophilus* GSTs and sequences from other nematodes showed that the pharyngeal gland cell sequences clustered with other sequences upregulated after infection. One (BUX.s01254.333) formed a cluster with other secreted and upregulated protein while the other (BUX.s00467.112) clustered with another secreted protein and two other upregulated proteins. This cluster includes the sequences that show the highest increases in expression during the infection of the host. Neither the pharyngeal gland cell GSTs, nor the secreted GSTs formed a single cluster (although the secreted GSTs were present as pairs in three clusters). These clusters were consistent in a neighbour-joining phylogenetic analysis (see Fig. S1 in the Supplementary material). These data suggest that a range of the GSTs present in *B. xylophilus* have been recruited independently to play a role in protection against host derived toxins and that the range of secreted GSTs has not evolved as a result of duplication of a single secreted ancestor.

Enzymatic and protective activity of GSTs involved in the host-parasite interaction

We next examined the biochemical activity of one of the pharyngeal gland cell GST sequences. The recombinant BUX.s00647.112 protein was cloned into an expression vector with an N-terminal His tag and purified from bacterial cell lysate, yielding a protein of approximately 25KDa, in agreement with the size predicted from the amino acid sequence (Fig. 2). The recombinant protein had glutathione transferase activity (using CDNB as a substrate) very similar to that observed for the positive control (Table 1). These data confirm that the BUX.s00647.112 protein is a functional GST.

Our previous data showed that several GSTs (including the BUX.s00647.112 sequence) are expressed in the pharyngeal gland cells, from where they could be secreted

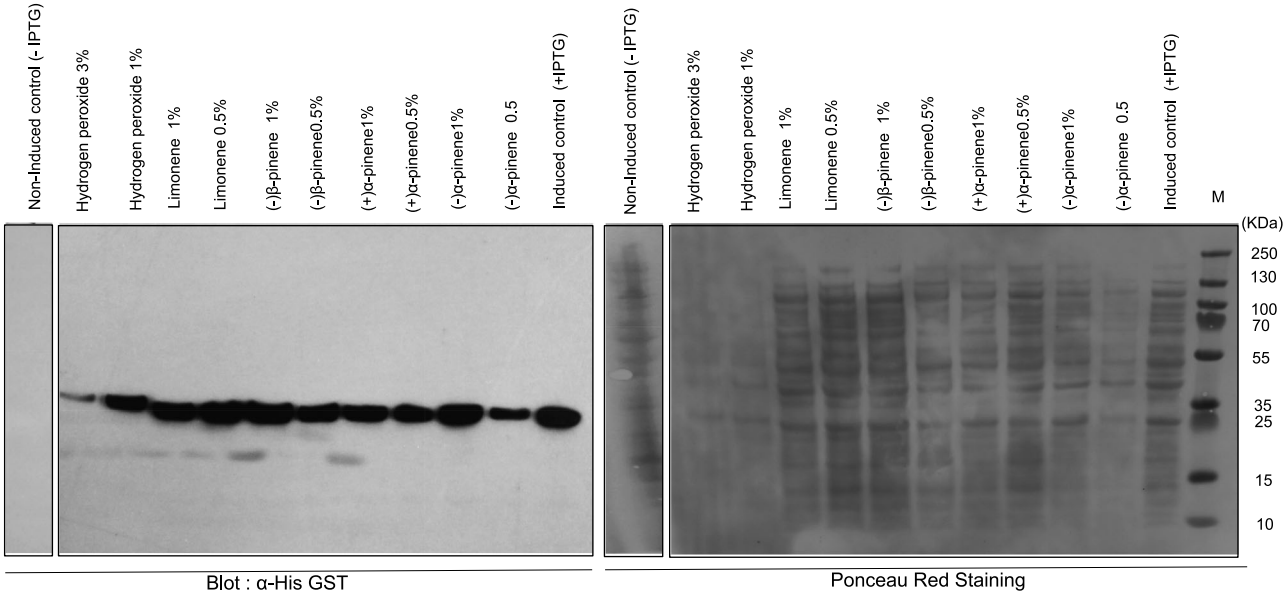

Fig. 2. The results of the immuno-detection of anti-Histag on the recombinant BUX.s00647.112 protein resistance assays. On the right, the Ponceau Red staining and on the left the results of the blot detected by chemiluminescence. M: protein ladder (GeneRuler, Thermofisher).

into the host. In addition, a larger scale proteomic analysis of *B. xylophilus* secreted proteins identified several peptides that could be derived from GST sequences (Shinya *et al*., 2013) further suggesting that GSTs form an important component of the *B. xylophilus* repertoire of secreted proteins. In keeping with this, we were able to detect GST activity (albeit at low levels) in secretions collected from *B. xylophilus* (Table 1). The RNAseq data suggest that it would have been possible to detect higher GST activity in secretions harvested from nematodes extracted from trees but technical limitations prevented us from attempting this analysis.

Table 1. Glutathione transferase activity results using CDNB as substrate (blank) in recombinant BUX.s00647.112 protein, *Bursaphelenchus xylophilus* protein extract and secretions. Each value is in the form mean ± SD.

Sample (CDNB as substrate)	GST activity (μmol ml^{-1} min^{-1})
GST activity in crude extracts of PWN proteins and secretions	
GST (control)	133.7 ± 62.3
PWN secretions	31.2 ± 1.9
PWN proteins	37.1 ± 0.2
GST activity in the recombinant BUX.s00647.112 protein	
GST (control)	1509.8 ± 73.4
Recombinant BUX.s00647.112	2096.3 ± 312.5

The GST protein control was provided in the kit (Sigma).

We next sought to analyse whether the *B. xylophilus* pharyngeal gland cell GST can provide protection against the toxins likely to be encountered by a nematode infecting a pine tree. Testing the function of the GST in pine trees is not possible due to technical limitations. We therefore compared the ability of bacterial cells in which the GST was either induced or not induced to grow in the presence of hydrogen peroxide and several terpenoid compounds. The peroxide was intended to represent the products of ROS, whilst the terpenoids were chosen to mimic toxic compounds likely to be present in an infected pine tree. In the presence of the GST, bacteria showed significantly higher growth in an environment with a (−) and (+)-α-pinene (−)-β-pinene, 0.5% limonene and up to 3% hydrogen peroxide (Fig. 3). There were no significant

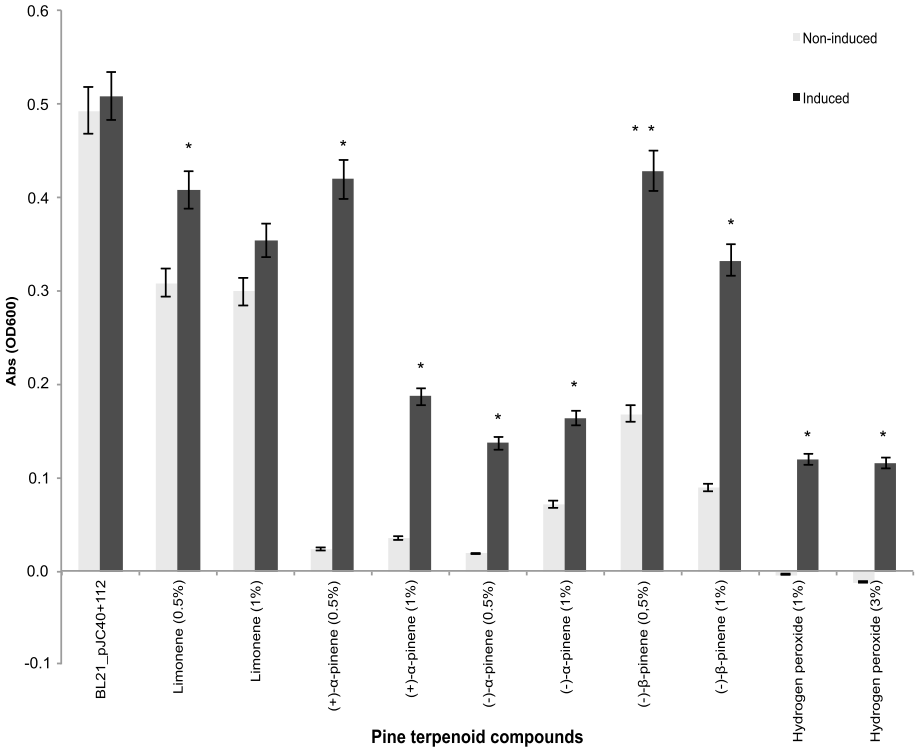

Fig. 3. Resistance test in BL21(DE3) cells. Induced *vs* non-induced BUX.s00647.112 protein using different pine terpenoid compounds and different concentrations of each (x-axis). The values on the y-axis correspond to values of absorbance (OD_{600}). The LB media was used to grow the bacteria. Protein expression was induced with 0.5 mM IPTG (see Materials and methods). Significant differences between induced and non-induced treatments were analysed by ANOVA ($^{*}P < 0.05$; $^{**}P < 0.01$).

differences in the 1% limonene treatment or in the control (induced *vs* non-induced). The difference in growth rate was most apparent in the presence of 0.5% (−)-β-pinene. A Western blot (Fig. 2) showed that the recombinant GST was present in all IPTG-induced samples while the non-induced bacterial cells showed no signal in the blot (Fig. 2).

These data confirm that *B. xylophilus* secretes functional GST proteins into the host, which may be important for allowing the nematode to overcome host defences. This may be a strategy that is widely used by plant-parasitic nematodes: a secreted GST has been identified from *M. incognita* (*Mi-gst-1*) that has been shown to promote infection of this nematode (Dubreuil *et al*., 2007) and which is also thought to function by protecting the nematode from host defences. Like the *B. xylophilus* sequence, the *M. incognita* GST is upregulated upon infection and expressed in the pharyngeal gland cells. GSTs also form a significant component of the strategy used by animal-parasitic nematodes to neutralise host defence responses. It is likely that GSTs used for internal metabolic processes have become adapted for a role in the host-parasite interaction in both plant- and animal-parasitic nematodes. Similar adaptation of housekeeping proteins for roles in parasitism in animal and plant parasites has been described previously with peroxiredoxins, glutathione peroxidases and lipid binding proteins all known to be deployed by plant parasites and animal parasites in order to provide protection from host defences (reviewed by Jasmer *et al*., 2003). Convergent evolution between animal- and plant-parasitic nematodes is therefore a recurring theme in terms of how they cope with host derived stresses.

Acknowledgements

This work was supported by the EU 7th Framework REPHRAME project (KBBE.2010.1.4-09) and by FEDER Funds through the Operational Programme for Competitiveness Factors – COMPETE and National Funds through FCT – Foundation for Science and Technology under the Strategic Projects PEst-C/AGR/UI0115/2011 and PEst-OE/AGR/UI0115/2014. ME is funded by the FCT (Fundação para a Ciência e a Tecnologia, IP) under the PhD grant (SFRH/BD/84541/2012). The James Hutton Institute receives funding from the Scottish Government. The authors thank Dr P.J.A. Cock for advice on this MS.

References

Azeez, S., Babu, R.O., Aykkal, R. & Narayanan, R. (2012). Virtual screening and *in vitro* assay of potential drug like inhibitors from spices against glutathione-S-transferase of filarial nematodes. *Journal of Molecular Modeling* 18, 151-163.

Bellafiore, S., Shen, Z.X., Rosso, M.N., Abad, P., Shih, P. & Briggs, S.P. (2008). Direct identification of the *Meloidogyne incognita* secretome reveals proteins with host cell reprogramming potential. *PLoS Pathogens* 4, e1000192.

Bendtsen, J.D., Nielsen, H., von Heijne, G. & Brunak, S. (2004). Improved prediction of signal peptides: SignalP 3.0. *Journal of Molecular Biology* 340, 783-795.

Brophy, P.M. & Barrett, J. (1990). Glutathione transferase in helminths. *Parasitology* 100, 345-349.

Brophy, P.M. & Pritchard, D.I. (1994). Parasitic-helminth glutathione S-transferases: an update on their potential targets for immuno- and chemotherapy. *Experimental Parasitology* 79, 89-96.

Campbell, A.M., Teesdale-Spittle, P.H., Barrett, J., Liebau, E., Jefferies, J.A. & Brophy, P.M. (2001). A common class of nematode glutathione S-transferase (GST) revealed by the theoretical proteome of the model organism *Caenorhabditis elegans*. *Comparative Biochemistry and Physiology Part B* 128, 701-708.

Cock, P.J.A., Chilton, J.M., Grüning, B., Johnson, J.E. & Soranzo, N. (2015). NCBI BLAST+ integrated into Galaxy. *GigaScience* 4, 39.

Cotton, J.A., Lilley, C.J., Jones, L.M., Kikuchi, T., Reid, A.J., Thorpe, P., Tsai, I.J., Beasley, H., Blok, V., Cock, P.J.A. *et al.* (2014). The genome and life-stage specific transcriptomes of *Globodera pallida* elucidate key aspects of plant parasitism by a cyst nematode. *Genome Biology* 15, R43.

Cwiklinski, K., de la Torre-Escudero, E., Trelis, M., Bernal, D., Dufresne, P.J., Brennan, G.P., O'Neill, S., Tort, J., Paterson, S., Marcilla, A. *et al.* (2015). The extracellular vesicles of the helminth pathogen, *Fasciola hepatica*: biogenesis pathways and cargo molecules involved in parasite pathogenesis. *Molecular and Cellular Proteomics* 12, 3258-3273.

Dowling, D.J., Hamilton, C.M., Donnelly, S., La Course, J., Brophy, P.M., Dalton, J. & O'Neill, S.M. (2010). Major secretory antigens of the helminth *Fasciola hepatica* activate a suppressive dendritic cell phenotype that attenuates Th17 cells but fails to activate Th2 immune responses. *Infection and Immunity* 78, 793-801.

Dubreuil, M., Magliano, E., Deleury, P., Abad, P. & Rosso, M.N. (2007). Transcriptome analysis of root-knot nematode functions induced in the early stages of parasitism. *New Phytologist* 176, 426-436.

Espada, M., Silva, A.C., Eves-van den Akker, S., Cock, P.J.A., Mota, M. & Jones, J.T. (2016). Identification and characterization of parasitism genes from the pinewood nematode *Bur-*

saphelenchus xylophilus reveals a multi-layered detoxification strategy. *Molecular Plant Pathology* 17, 286-295.

Faria, J.M.S., Sena, I., Vieira da Silva, I., Ribeiro, B., Barbosa, P., Ascensão, L., Bennett, R.N., Mota, M. & Figueiredo, A.C.F. (2015). *In vitro* co-cultures of *Pinus pinaster* with *Bursaphelenchus xylophilus*: a biotechnological approach to study pine wilt disease. *Planta* 241, 1325-1336.

Frova, C. (2006). Glutathione transferases in the genomics era: new insights and perspectives. *Biomolecular Engineering* 23, 149-169.

Fukuda, K. (1997). Physiological process of the symptom development and resistance mechanism in pine wilt disease. *Journal of Forest Research* 2, 171-181.

Gouy, M., Guindon, S. & Gascuel, O. (2010). SeaView version 4: a multiplatform graphical user interface for sequence alignment and phylogenetic tree building. *Molecular Biology and Evolution* 27, 221-224.

Haegeman, A., Jacob, J., Vanholme, B., Kyndt, T., Mitreva, M. & Gheysen, G. (2009). Expressed sequence tags of the peanut pod nematode *Ditylenchus africanus*: the first transcriptome analysis of an anguinid nematode. *Molecular Biochemical Parasitology* 167, 32-40.

Haegeman, A., Joseph, S. & Gheysen, G. (2011). Analysis of the transcriptome of the root lesion nematode *Pratylenchus coffeae* generated by 454 sequencing technology. *Molecular Biochemical Parasitology* 178, 7-14.

Jacob, J., Mitreva, M., Vanholme, B. & Gheysen, G. (2008). Exploring the transcriptome of the burrowing nematode *Radopholus similis*. *Molecular Genetics and Genomics* 280, 1-17.

Jasmer, D.P., Goverse, A. & Smant, G. (2003). Parasitic nematode interactions with mammals and plants. *Annual Review of Phytopathology* 41, 245-270.

Jones, P., Binns, D., Chang, H., Fraser, M., Li, W., McAnulla, C., McWilliam, H., Maslen, J., Mitchell, A., Nuka, G. *et al.* (2014). InterProScan 5: genome-scale protein function classification. *Bioinformatics* 30, 1236-1240.

Kikuchi, T., Jones, J.T., Aikawa, T., Kosaka, H. & Ogura, N. (2004). A family of glycosyl hydrolase family 45 cellulases from the pinewood nematode *Bursaphelenchus xylophilus*. *FEBS Letters* 572, 201-205.

Kikuchi, T., Cotton, J.A., Dalzell, J.J., Hasegawa, K., Kanzaki, N., McVeigh, P., Takanashi, T., Tsai, I.J., Assefa, S.A., Cock, P.J.A. *et al.* (2011). Genomic insights into the origin of parasitism in the emerging plant pathogen *Bursaphelenchus xylophilus*. *PLoS Pathogens* 7, e1002219.

Kuroda, K. (1991). Mechanism of cavitation development in the pine wilt disease. *European Journal of Forest Pathology* 21, 82-89.

Kuroda, K., Yamada, T. & Ito, S. (1991). *Bursaphelenchus xylophilus* induced pine wilt: factors associated with resistance. *European Journal of Forest Pathology* 21, 430-438.

LaCourse, E.J., Perally, S., Morphew, R.M., Moxon, J.V., Prescott, M., Dowling, D.J., O'Neill, S.M., Kipar, A., Hetzel, U., Hoey, E. *et al.* (2012). The sigma class glutathione transferase from the liver fluke *Fasciola hepatica*. *PLoS Neglected Tropical Diseases* 6, e1666.

Matoušková, P., Vokřál, I., Lamka, J. & Skálová, L. (2016). The role of xenobiotic-metabolizing enzymes in anthelmintic deactivation and resistance in helminths. *Trends in Parasitology*, in press. DOI:10.1016/j.pt.2016.02.004.

Precious, W.Y. & Barrett, J. (1989). Xenobiotic metabolism in helminths. *Parasitology Today* 5, 156-160.

Shinya, R., Morisaka, H., Kikuchi, T., Takeuchi, Y., Ueda, M. & Futai, K. (2013). Secretome analysis of the pine wood nematode *Bursaphelenchus xylophilus* reveals the tangled roots of parasitism and its potential for molecular mimicry. *PLoS ONE* 8, e67377.

Torres-Rivera, A. & Landa, A. (2008). Gluthathione transferases from parasites: a biochemical view. *Acta Tropica* 105, 99-112.

van Rossum, A.J., Jefferies, J.R., Rijsewijk, F.A.M., LaCourse, E.J., Teesdale-Spittle, P., Barrett, J., Tait, A. & Brophy, P.M. (2004). Binding of hematin by a new class of glutathione transferase from the blood-feeding parasitic nematode *Haemonchus contortus*. *Infection and Immunity* 72, 2780-2790.

Supplementary material

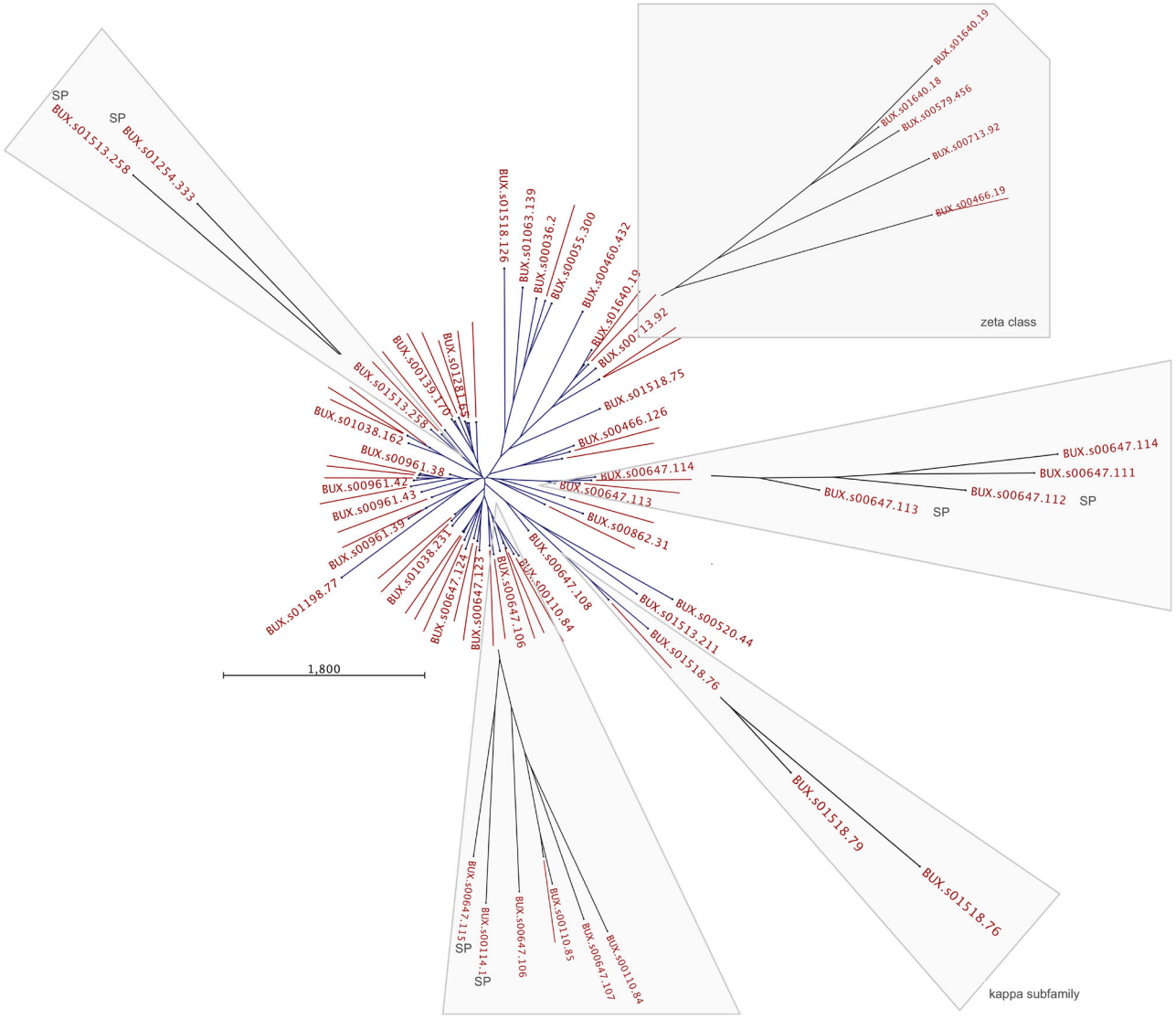

Fig. S1. Neighbour-joining phylogenetic tree of all 70 protein sequences from *Bursaphelenchus xylophilus*. The highlighted clusters in grey boxes represent the kappa subfamily, the zeta class and the clusters with the protein of interest (BUX.s00647.112) and the proteins with predicted signal peptide. This tree confirms that the clusters are not an artefact of the maximum-likelihood phylogenetic tree. This figure is published in colour in the online edition of this journal, which can be accessed *via* http://booksandjournals.brillonline.com/content/journals/15685411.

Table S1. Protein domains predicted for all 70 putative GSTs from *Bursaphelenchus xylophilus*. Each domain is represented by the InterProScan identification code and for some of the proteins the family was identified.

Gene code*	Protein family	Number domain 1	Number domain 2	Number domain 3
BUX.c04223.1	None	IPR010987 Glutathione S-transferase, C-terminal-like	IPR004046 Glutathione S-transferase, C-terminal	
BUX.c09083.1	None	IPR012336 Thioredoxin-like fold	IPR004045 Glutathione S-transferase, N-terminal	IPR010987 Glutathione S-transferase, C-terminal-like
BUX.s00110.84	None	IPR012336 Thioredoxin-like fold	IPR004045 Glutathione S-transferase, N-terminal	IPR010987 Glutathione S-transferase, C-terminal-like
BUX.s00110.85	None	IPR012336 Thioredoxin-like fold	IPR004045 Glutathione S-transferase, N-terminal	IPR010987 Glutathione S-transferase, C-terminal-like
BUX.s00114.1	None	IPR012336 Thioredoxin-like fold	IPR004045 Glutathione S-transferase, N-terminal	IPR010987 Glutathione S-transferase, C-terminal-like
BUX.s00116.427	Failed axon connections IPR026928	IPR012336 Thioredoxin-like fold	IPR010987 Glutathione S-transferase, C-terminal-like	IPR004046 Glutathione S-transferase, C-terminal
BUX.s00116.457	None	IPR012336 Thioredoxin-like fold	IPR004045 Glutathione S-transferase, N-terminal	IPR010987 Glutathione S-transferase, C-terminal-like
BUX.s00116.338	None	IPR012336 Thioredoxin-like fold	IPR004045 Glutathione S-transferase, N-terminal	IPR010987 Glutathione S-transferase, C-terminal-like
BUX.s00139.169	None	IPR012336 Thioredoxin-like fold	IPR004045 Glutathione S-transferase, N-terminal	IPR010987 Glutathione S-transferase, C-terminal-like
BUX.s00139.170	None	IPR012336 Thioredoxin-like fold	IPR004045 Glutathione S-transferase, N-terminal	IPR010987 Glutathione S-transferase, C-terminal-like
BUX.s00460.83	None	IPR012336 Thioredoxin-like fold	IPR004045 Glutathione S-transferase, N-terminal	IPR010987 Glutathione S-transferase, C-terminal-like
BUX.s00466.126	None	IPR012336 Thioredoxin-like fold	IPR004045 Glutathione S-transferase, N-terminal	IPR010987 Glutathione S-transferase, C-terminal-like
BUX.s00466.66	None	IPR012336 Thioredoxin-like fold	IPR004045 Glutathione S-transferase, N-terminal	IPR010987 Glutathione S-transferase, C-terminal-like
BUX.s00631.40	None	IPR012336 Thioredoxin-like fold	IPR004045 Glutathione S-transferase, N-terminal	IPR010987 Glutathione S-transferase, C-terminal-like
BUX.s00647.107	None	IPR012336 Thioredoxin-like fold	IPR004045 Glutathione S-transferase, N-terminal	IPR010987 Glutathione S-transferase, C-terminal-like
BUX.s00647.123	None	IPR012336 Thioredoxin-like fold	IPR004045 Glutathione S-transferase, N-terminal	
BUX.s00647.116	None	IPR012336 Thioredoxin-like fold	IPR004045 Glutathione S-transferase, N-terminal	
BUX.s00647.121	None	IPR012336 Thioredoxin-like fold	IPR004045 Glutathione S-transferase, N-terminal	IPR010987 Glutathione S-transferase, C-terminal-like
BUX.s00647.112	None	IPR012336 Thioredoxin-like fold	IPR004045 Glutathione S-transferase, N-terminal	IPR010987 Glutathione S-transferase, C-terminal-like
BUX.s00647.118	None	IPR012336 Thioredoxin-like fold	IPR004045 Glutathione S-transferase, N-terminal	IPR010987 Glutathione S-transferase, C-terminal-like
BUX.s00647.119	None	IPR012336 Thioredoxin-like fold	IPR004045 Glutathione S-transferase, N-terminal	IPR010987 Glutathione S-transferase, C-terminal-like
BUX.s00647.113	None	IPR012336 Thioredoxin-like fold	IPR004045 Glutathione S-transferase, N-terminal	
BUX.s00647.126	None	IPR012336 Thioredoxin-like fold	IPR004045 Glutathione S-transferase, N-terminal	IPR010987 Glutathione S-transferase, C-terminal-like

Table S1. (Continued.)

Gene code*	Protein family	Number domain 1	Number domain 2	Number domain 3
BUX.s00647.124	None	IPR012336 Thioredoxin-like fold	IPR004045 Glutathione S-transferase, N-terminal	IPR010987 Glutathione S-transferase, C-terminal-like
BUX.s00647.108	None	IPR012336 Thioredoxin-like fold	IPR004045 Glutathione S-transferase, N-terminal	
BUX.s00647.115	None	IPR012336 Thioredoxin-like fold	IPR004045 Glutathione S-transferase, N-terminal	
BUX.s00647.111	None	IPR012336 Thioredoxin-like fold	IPR004045 Glutathione S-transferase, N-terminal	IPR010987 Glutathione S-transferase, C-terminal-like
BUX.s00647.110	None	IPR012336 Thioredoxin-like fold	IPR004045 Glutathione S-transferase, N-terminal	IPR010987 Glutathione S-transferase, C-terminal-like
BUX.s00647.125	None	IPR012336 Thioredoxin-like fold	IPR004045 Glutathione S-transferase, N-terminal	IPR010987 Glutathione S-transferase, C-terminal-like
BUX.s00647.122	None	IPR012336 Thioredoxin-like fold	IPR004045 Glutathione S-transferase, N-terminal	IPR010987 Glutathione S-transferase, C-terminal-like
BUX.s00862.31	None	IPR012336 Thioredoxin-like fold	IPR004045 Glutathione S-transferase, N-terminal	
BUX.s00961.40	None	IPR012336 Thioredoxin-like fold	IPR004045 Glutathione S-transferase, N-terminal	IPR010987 Glutathione S-transferase, C-terminal-like
BUX.s00961.38	None	IPR012336 Thioredoxin-like fold	IPR004045 Glutathione S-transferase, N-terminal	
BUX.s00961.36	None	IPR012336 Thioredoxin-like fold	IPR004045 Glutathione S-transferase, N-terminal	IPR010987 Glutathione S-transferase, C-terminal-like
BUX.s00961.42	None	IPR012336 Thioredoxin-like fold	IPR004045 Glutathione S-transferase, N-terminal	IPR010987 Glutathione S-transferase, C-terminal-like
BUX.s00961.37	None	IPR012336 Thioredoxin-like fold	IPR004045 Glutathione S-transferase, N-terminal	IPR010987 Glutathione S-transferase, C-terminal-like
BUX.s00961.43	None	IPR012336 Thioredoxin-like fold	IPR004045 Glutathione S-transferase, N-terminal	IPR010987 Glutathione S-transferase, C-terminal-like
BUX.s00961.41	None	IPR012336 Thioredoxin-like fold	IPR004045 Glutathione S-transferase, N-terminal	IPR010987 Glutathione S-transferase, C-terminal-like
BUX.s00983.23	None	IPR012336 Thioredoxin-like fold	IPR004045 Glutathione S-transferase, N-terminal	IPR010987 Glutathione S-transferase, C-terminal-like
BUX.s01038.67	None	IPR012336 Thioredoxin-like fold	IPR004045 Glutathione S-transferase, N-terminal	
BUX.s01038.162	None	IPR012336 Thioredoxin-like fold	IPR004045 Glutathione S-transferase, N-terminal	IPR010987 Glutathione S-transferase, C-terminal-like
BUX.s01038.66	None	IPR010987 Glutathione S-transferase, C-terminal-like	IPR004046 Glutathione S-transferase, C-terminal	
BUX.s01038.231	None	IPR012336 Thioredoxin-like fold	IPR004045 Glutathione S-transferase, N-terminal	IPR010987 Glutathione S-transferase, C-terminal-like
BUX.s01092.134	None	IPR012336 Thioredoxin-like fold	IPR004045 Glutathione S-transferase, N-terminal	IPR010987 Glutathione S-transferase, C-terminal-like
BUX.s01254.333	None	IPR012336 Thioredoxin-like fold	IPR004045 Glutathione S-transferase, N-terminal	IPR010987 Glutathione S-transferase, C-terminal-like
BUX.s01254.332	None	IPR012336 Thioredoxin-like fold	IPR004045 Glutathione S-transferase, N-terminal	IPR010987 Glutathione S-transferase, C-terminal-like
BUX.s01281.65	None	IPR012336 Thioredoxin-like fold	IPR004045 Glutathione S-transferase, N-terminal	IPR010987 Glutathione S-transferase, C-terminal-like

Table S1. (Continued.)

Gene code*	Protein family	Number domain 1	Number domain 2	Number domain 3
BUX.s01281.64	None	IPR012336 Thioredoxin-like fold	IPR004045 Glutathione S-transferase, N-terminal	IPR010987 Glutathione S-transferase, C-terminal-like
BUX.s01368.1	None	IPR012336 Thioredoxin-like fold	IPR004045 Glutathione S-transferase, N-terminal	IPR010987 Glutathione S-transferase, C-terminal-like
BUX.s01513.258	None	IPR012336 Thioredoxin-like fold	IPR004045 Glutathione S-transferase, N-terminal	IPR010987 Glutathione S-transferase, C-terminal-like
BUX.s01518.75	None	IPR012336 Thioredoxin-like fold	IPR010987 Glutathione S-transferase, C-terminal-like	IPR004046 Glutathione S-transferase, C-terminal
BUX.s00520.44	None	IPR012336 Thioredoxin-like fold	IPR001853 DSBA-like thioredoxin domain	
BUX.s00647.114	None	IPR010987 Glutathione S-transferase, C-terminal-like		
BUX.s01513.211	None	IPR012336 Thioredoxin-like fold	IPR001853 DSBA-like thioredoxin domain	
BUX.s01518.79	None	IPR001853 DSBA-like thioredoxin domain	IPR012336 Thioredoxin-like fold	
BUX.s01518.76	HCCA isomerase/ glutathione S-transferase kappa (IPR014440)	IPR012336 Thioredoxin-like fold	IPR001853 DSBA-like thioredoxin domain	
BUX.s00036.2	None	IPR010987 Glutathione S-transferase, C-terminal-like	IPR004046 Glutathione S-transferase, C-terminal	
BUX.s00055.300	None	IPR012336 Thioredoxin-like fold	IPR010987 Glutathione S-transferase, C-terminal-like	IPR004046 Glutathione S-transferase, C-terminal
BUX.s00460.432	None	IPR2109 Glutaredoxin	IPR012336 Thioredoxin-like fold	IPR004045 Glutathione S-transferase, N-terminal
BUX.s00466.18	Maleylacetoacetate isomerase (IPR005955)	IPR005955 Maleyacetoacetate isomerase	IPR012336 Thioredoxin-like fold	IPR004045 Glutathione S-transferase, N-terminal
BUX.s00466.19	Maleylacetoacetate isomerase (IPR005955)	IPR005955 Maleyacetoacetate isomerase	IPR012336 Thioredoxin-like fold	IPR004045 Glutathione S-transferase, N-terminal
BUX.s00579.456	Maleylacetoacetate isomerase (IPR005955)	IPR005955 Maleyacetoacetate isomerase	IPR012336 Thioredoxin-like fold	IPR004045 Glutathione S-transferase, N-terminal
Bux.s00647.106	None	IPR012336 Thioredoxin-like fold	IPR010987 Glutathione S-transferase, C-terminal-like	
BUX.s00713.92	Maleylacetoacetate isomerase (IPR005955)	IPR005955 Maleyacetoacetate isomerase	IPR012336 Thioredoxin-like fold	IPR004045 Glutathione S-transferase, N-terminal

Table S1. (Continued.)

Gene code*	Protein family	Number domain 1	Number domain 2	Number domain 3
BUX.s00961.39	None	IPR010987 Glutathione S-transferase, C-terminal-like		
BUX.s01063.139	None	IPR010987 Glutathione S-transferase, C-terminal-like	IPR004046 Glutathione S-transferase, C-terminal	
BUX.s01198.77	None	IPR012336 Thioredoxin-like fold	IPR010987 Glutathione S-transferase, C-terminal-like	
BUX.s01518.126	None	IPR012336 Thioredoxin-like fold	IPR010987 Glutathione S-transferase, C-terminal-like	IPR004046 Glutathione S-transferase, C-terminal
BUX.s01640.19	None	IPR012336 Thioredoxin-like fold	IPR004045 Glutathione S-transferase, N-terminal	IPR010987 Glutathione S-transferase, C-terminal-like
BUX.s01640.18	Maleylacetoacetate isomerase (IPR005955)	IPR012336 Thioredoxin-like fold	IPR004045 Glutathione S-transferase, N-terminal	IPR010987 Glutathione S-transferase, C-terminal-like

* According to PWN gene calls of the genome (version 1.2); available in GeneDB (www.genedb.org/Homepage/Bxylophilus).